ORIGINAL PAPER



Direct Formation of Lubricious and Wear-Protective Carbon Films from Phosphorus- and Sulfur-Free Oil-Soluble Additives

Blake Johnson¹ · Hongxing Wu^{1,4} · Michael Desanker² · David Pickens¹ · Yip-Wah Chung³ · Q. Jane Wang¹

Received: 19 August 2017 / Accepted: 26 October 2017 © Springer Science+Business Media, LLC 2017

Abstract

Extreme pressure (EP) lubricant additives form protective tribofilms at the site of contact using the heat and pressure of contact and relative motion. Common EP additives contain undesirable elements such as phosphorus and sulfur. A novel EP lubricant additive, which contains no phosphorus and sulfur, is presented for generating lubricious carbon films. The additive consists of a surface-active molecule with a metastable cycloalkane ring, which dissociates readily during tribological contact to form lubricious carbon films. Friction and wear performance of PAO4 with this additive under a range of loads and speeds were shown to be superior to that without the additive. Optical and scanning electron microscopy and Raman spectroscopy were used to analyze the tribofilms formed on post-test contact surfaces, providing direct evidence for the formation of carbon films. Quantitative kinetics for the carbon tribofilm formation was analyzed as a function of temperature and stress, from which the activation energy for carbon tribofilm formation was obtained.

Keywords Extreme pressure additives · Antiwear additives · Additive deposition

1 Introduction

Transportation accounts for 28% of energy consumption globally [1], and improved lubrication in transportation systems can significantly reduce oil consumption and the associated CO₂ emission [2–5]. Each 1% improvement in fuel economy of light-duty vehicles lowers fuel consumption by 100,000 barrels of oil per day in the USA alone [6]. Lubrication technology is also crucial in the reliability and lifetime of vehicles and can reduce the toxicity of engine exhaust [7]. Overall, it has been reported that 1–1.4% of the

- GDP can be saved through research and implementation of new lubrication technology [8, 9]. Under ideal engine operation conditions, lubricants work
- by forming a fluid film that hydrodynamically supports the load between mating surfaces. However, during starting and stopping of the engine, reduced engine speed prevents the lubricant from forming a continuous fluid film between mating surfaces, and asperities on the mating surfaces come into direct contact. This condition is known as boundary lubrication (BL) or in the case where some of the load is supported by the fluid, it is known as mixed lubrication (ML). These conditions lead to high friction and wear during engine operation. BL and ML are especially important for hybrid vehicles, whose engines start and stop each time the drive train switches to and from battery power. Also, many new vehicles implement 'start-stop' systems, which reduce fuel consumption by automatically shutting the engine off when the vehicle is motionless [10]. Overall, lubricant design for modern engine systems must give due consideration to the frequent occurrence of BL and ML conditions [11].

Lubricant additives serve many purposes from corrosion resistance and contamination control to friction reduction and wear protection [12]. Extreme pressure (EP) additives are a class of additives designed specifically to protect surfaces in BL and ML conditions. Most EP additives work by

☐ Yip-Wah Chung ywchung@northwestern.edu

Published online: 20 November 2017

- Q. Jane Wang qwang@northwestern.edu
- Department of Mechanical Engineering, Northwestern University, Evanston, IL 60201, USA
- Department of Chemistry, Northwestern University, Evanston, IL 60201, USA
- Department of Materials Science and Engineering, Northwestern University, Evanston, IL 60201, USA
- ⁴ Key Laboratory of Education Ministry for Modern Design and Rotor Bearing Systems, Xi'an Jiaotong University, Xi'an 710049, People's Republic of China



harnessing the energetic and chemically active environment at asperity contacts to induce chemical reactions, forming lubricious and protective layers on surfaces, known as tribofilms. The most common class of EP additives is zinc dialkyl-dithio-phosphate (ZDDP). ZDDP generates an effective and strong phosphate tribofilm that reduces friction and wear. Despite its effectiveness, the use of ZDDP has been increasingly discouraged, because phosphorus- and sulfurcontaining residues from the decomposition of ZDDP can accumulate in catalytic converters [13, 14], causing permanent damage [15–18]. An alternative sulfur- and phosphorus-free lubricant additive is needed.

Diamond-like carbon (DLC) is a catch-all term for amorphous carbon materials containing a mixture of hydrogen, sp²- and sp³-bonded carbon, and other elements such as nitrogen and metals. It has been used industry-wide in protective overcoats for computer disk drives since the early 1990s [19–23]. DLC has been shown to exhibit excellent tribological performance, with ultra-low friction behavior attributed to lubricious graphitic films that slide between surfaces [24, 25]. Delamination, poor adhesion, and high internal stresses are among some of the challenges for DLC coatings [26]. For automotive applications, a major drawback of DLC is that it must be deposited on surfaces as a pre-treatment during manufacturing. Once the coating is worn away, it cannot be replenished without complete disassembly of the system. Further, DLC-coated surfaces are chemically inert and therefore have poor compatibility with conventional lubricant additives [27-29].

One may approach the problem with DLC discussed in the preceding paragraph by producing carbon tribofilms in situ, rather than relying solely on a static DLC coating. Carbon tribofilms are known to form when hydrocarbons dissociate at asperity contacts [30, 31]. Properties of carbon tribofilms vary widely, and they can have a strong positive or negative affect on friction and wear. Under certain conditions, carbon tribofilms can be as effective as ZDDP tribofilms [31–33]. Carbon tribofilms are generally formed through a distinct chemical pathway [30]. First, hydrocarbon adsorbed near the contact undergoes tribochemical oxidation, resulting in high molecular weight polymers that precipitate out of the fluid. The hydrocarbon macromolecules then dehydrogenate into amorphous carbon, and continued frictional energy input causes further transformation to graphitic carbon films. Graphitic carbon reduces friction and wear by providing a soft, low-shear stress buffer material between mating surfaces [30, 34, 35]. Erdemir and coworkers developed a catalytically active coating based on nanoscale copper that facilitates the dissociation of hydrocarbon base fluid into such lubricious carbon tribofilms [32]. Additional studies have discovered carbon-based tribofilms with carbon derived from base fluids and carbon-containing vapors [14, 36-41]. These studies represent a promising

alternative to conventional ZDDP additives. However, the surfaces presented in these studies are often modified to create catalytically active environment necessary for lubricious carbon tribofilm formation. If such surface modification is worn away, or depleted at the locations where such a film is demanded, the process to form lubricious carbon films cannot be reactivated without component disassembly and coating re-deposition.

The work reported in this paper represents a novel technology for EP lubricant additives designed to provide replenishable carbon films in situ at the location of contact, without any pre-treatment of the contact surfaces. The additive contains no phosphorus and sulfur and is designed to undergo a tribochemical reaction that produces a lubricious carbon film. An example molecule embodying this concept has been selected, and its effectiveness is demonstrated through tribotesting and surface analysis. Analysis of the tribochemistry and lubrication mechanisms will then be discussed.

2 Materials and Methods

The carbon tribofilm precursor molecule must be soluble in base oil and should have two key moieties. The first is a three- or four-carbon cycloalkane, which is metastable because the carbon–carbon bonds within the cycloalkane are highly strained and are therefore prone to dissociation at relatively low temperatures and pressures, compared to linear hydrocarbons [41–43]. The second moiety is a surfaceactive group that binds the molecule to the surface via dipole forces, allowing thermal energy due to frictional heating to couple directly to the precursor molecule [30]. Carboxylic (-COOH) and alcohol (-OH) groups are examples of such surface-active species. In this work, we chose cyclopropanecarboxylic acid (C₃H₅CO₂H, CPCa), shown in Fig. 1, as our carbon precursor, which is commercially available.

Ball-on-disk tribotests were performed under fully flooded lubrication in simple sliding for 30 min using a CETR UMT-2 tribometer. The ball and disk were 52100

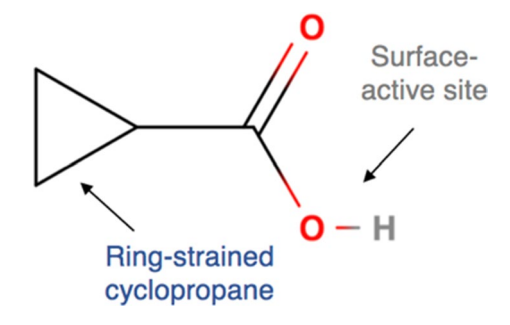


Fig. 1 CPCa molecule containing a metastable carbon ring (cyclopropane) as the carbon source and a surface-active group (-COOH) that provides adsorption to the surface



Tribology Letters (2018) 66:2 Page 3 of 13 ☑



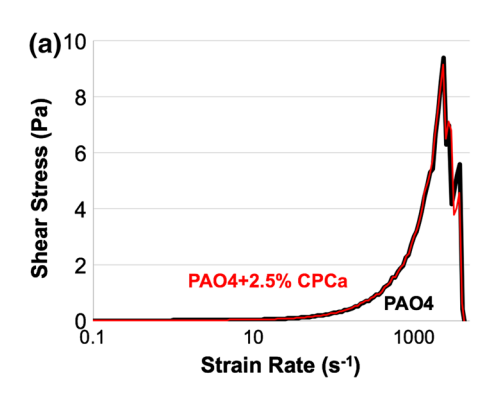
Fig. 2 Picture of PAO4 and PAO4 + 2.5 wt% CPCa after sitting for 48 h. No phase separation was observed

Table 1 Test conditions for all tribological tests

Test conditions	
Lubricants	PAO4, PAO4 + 2.5 wt% CPCa
Load (N)	3, 5, 10, 15, 20
Hertzian pressure (GPa)	0.8, 0.9, 1.1, 1.3, 1.4
Speed (mm s ⁻¹)	25, 50, 100, 200
Time (min)	30
Environment	1 Atm, 25 °C
Materials	52100 bearing steel

bearing steel with a hardness of 60 HRC, polished to root-mean-square roughness (R_{RMS}) of 50 nm and 100 nm, respectively. Two lubricant samples were tested: a neat polyalpha-olefin base fluid (PAO4) and PAO4 + 2.5 wt% CPCa. At this concentration, CPCa is fully miscible with PAO4. No phase separation was observed, even after leaving the fluid still for 48 h (Fig. 2).

Fig. 3 Shear stress (a) and dynamic viscosity (b) of PAO4 influenced by strain rate with and without the addition of 2.5 wt% CPCa



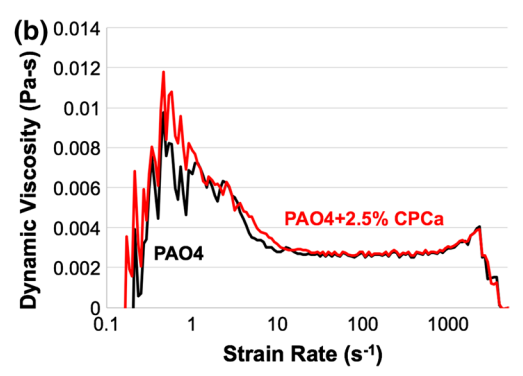




Table 1 shows the test matrix consisting of 20 test conditions at different speed load combinations. Tests conditions were selected to cover the BL and ML regimes, based on film thickness predictions made using contact modeling software [44–51]. The software model also predicts the maximum asperity flash temperature and the percentage of the total load supported by asperities (solid). Friction force was measured in real time during tribotesting, while wear of the ball was evaluated after testing using white light interferometry. The wear rate is defined as the volume removed from the surface divided by the distance traveled.

Post-test surfaces were rinsed gently with hexane and analyzed using optical microscopy and scanning electron microscopy (SEM). Cross-sectional SEM, through focused ion beam milling (FIB), along with energy-dispersive X-ray spectroscopy (EDS), was performed on select surfaces. Raman spectroscopy was performed using a laser wavelength of 514.5 nm and 45 s scan time. Two features in the Raman spectrum, the D and G bands, around 1360 and 1560 cm⁻¹, respectively, have been extensively discussed in the literature. The G band corresponds to carbon sp² bond stretching within the crystalline graphite structure. The D band is linked to vibration at the edges of graphite or graphene structures and is associated with disordered, noncrystalline carbon morphology [52].

3 Results

3.1 Fluid Dynamics

Before assessing the BL and ML performance of CPCa, the effect of the additive on the lubricant's fluid dynamics was assessed. CPCa was found to be readily oil-soluble, and Fig. 3 shows that the addition of 2.5% of CPCa has no obvious influence on the shear stress–strain rate behavior and only causes a slight increase in viscosity at low strain rates. Carboxylic acids are routinely used as additives in lubricant formulations, and this compatibility should be expected.

3.2 Friction and Wear Performance

X

Figure 4 presents wear rates obtained from 20 tests using PAO4 as lubricant and 20 tests using PAO4 + CPCa. When averaged over all 20 tests, PAO4 + CPCa results in a 93% reduction in wear rate compared with neat PAO4.

Figure 5 shows results on coefficient of friction, averaged over 30 min, obtained from 20 tests using PAO4 as lubricant and 20 tests using PAO4 + CPCa. When averaged over all 20 tests, PAO4 + CPCa yields an 18% reduction in coefficient of friction compared with neat PAO4.

Figure 6 shows the time evolution of friction coefficient for a few representative tests. The friction curves for the PAO4 + CPCa fluid have two notable features. First, they exhibit an exponential decay of friction from the neat PAO4 value to a lower steady-state value, within the first few minutes of the test. The shape of the curve is similar to what has been observed previously for other tribofilm-forming additives [53–56]. Second, for tests conducted at larger loads and lower speeds, as shown in Fig. 4c, d, the friction coefficient trend is disrupted with a sudden jump after a few minutes of tribotesting [57]. All friction versus time plots for the PAO4 + CPCa fluid follow either the shape of Fig. 6a, b or Fig. 6c, d.

3.3 Performance Factors

Figure 7 shows a series of interpolated maps plotting the trends of wear rate and average friction from the 20 experiments using PAO4 + CPCa. Black circles indicate points where the tests were actually performed. Best performance in friction and wear occurs at low loads and high speeds. According to the Stribeck curve, these conditions are associated with greater load support from the fluid [58]. One can calculate the percentage of load supported by the solid for the 20 tests using PAO4 + CPCa, as shown in Fig. 7c. Figure 7d shows how the wear rate correlates with this percentage (contact load ratio). The wear rate remains constant at contact load ratio between 5 and 95%, increasing rapidly when the two surfaces come into complete contact and there is no load support by the fluid.

3.4 Tribofilm Morphology

Figure 8 shows several surface observations on the disk surface after testing with PAO4 + CPCa at 10 N load and 200 mm s⁻¹. Figure 6a shows an optical micrograph of the wear scar with colored deposits. The colorful spots and blank regions are due to varying thicknesses of the carbon film [59]. Figure 6b shows a series of Raman spectra taken

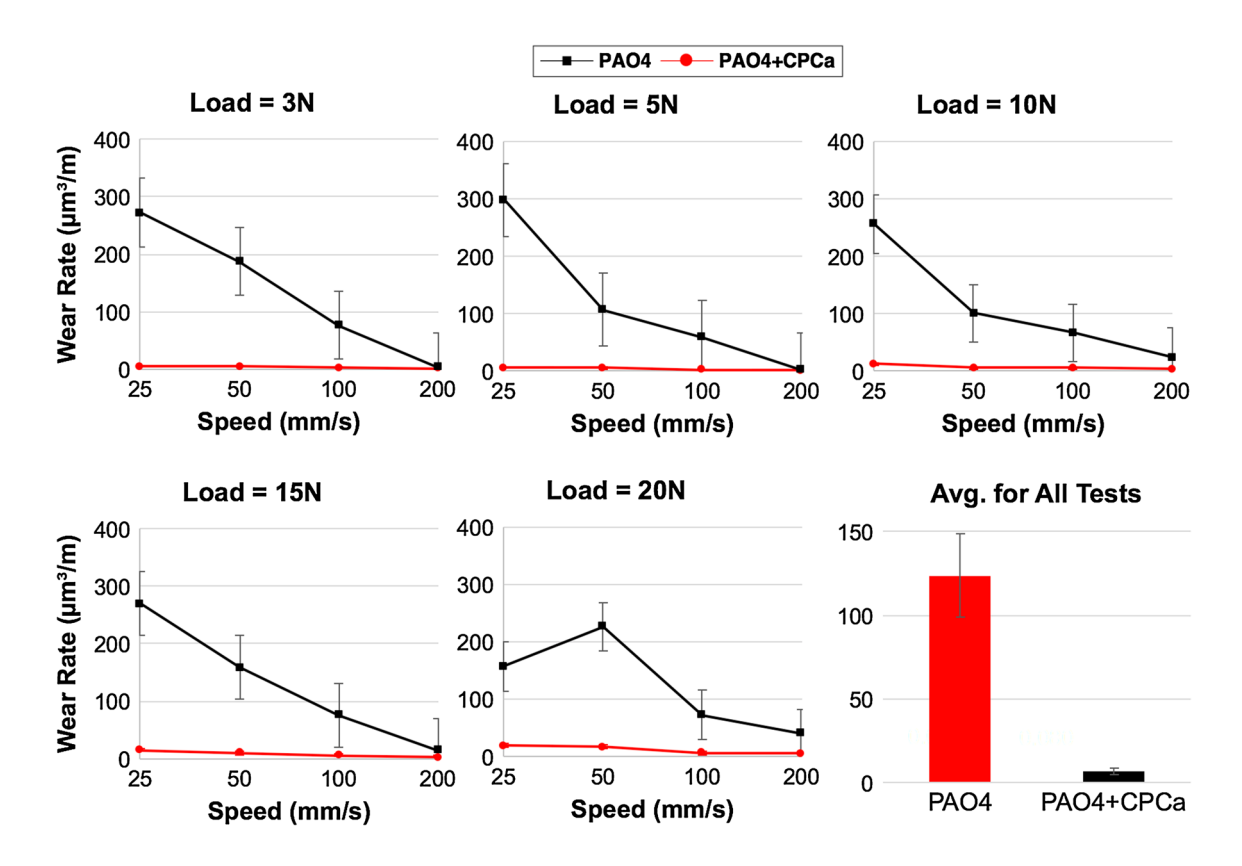


Fig. 4 Wear rates for tests using PAO4 and PAO4 + CPCa as lubricants, and a comparison of wear rates averaged over all 20 tests using these two lubricants



Tribology Letters (2018) 66:2 Page 5 of 13 ☑

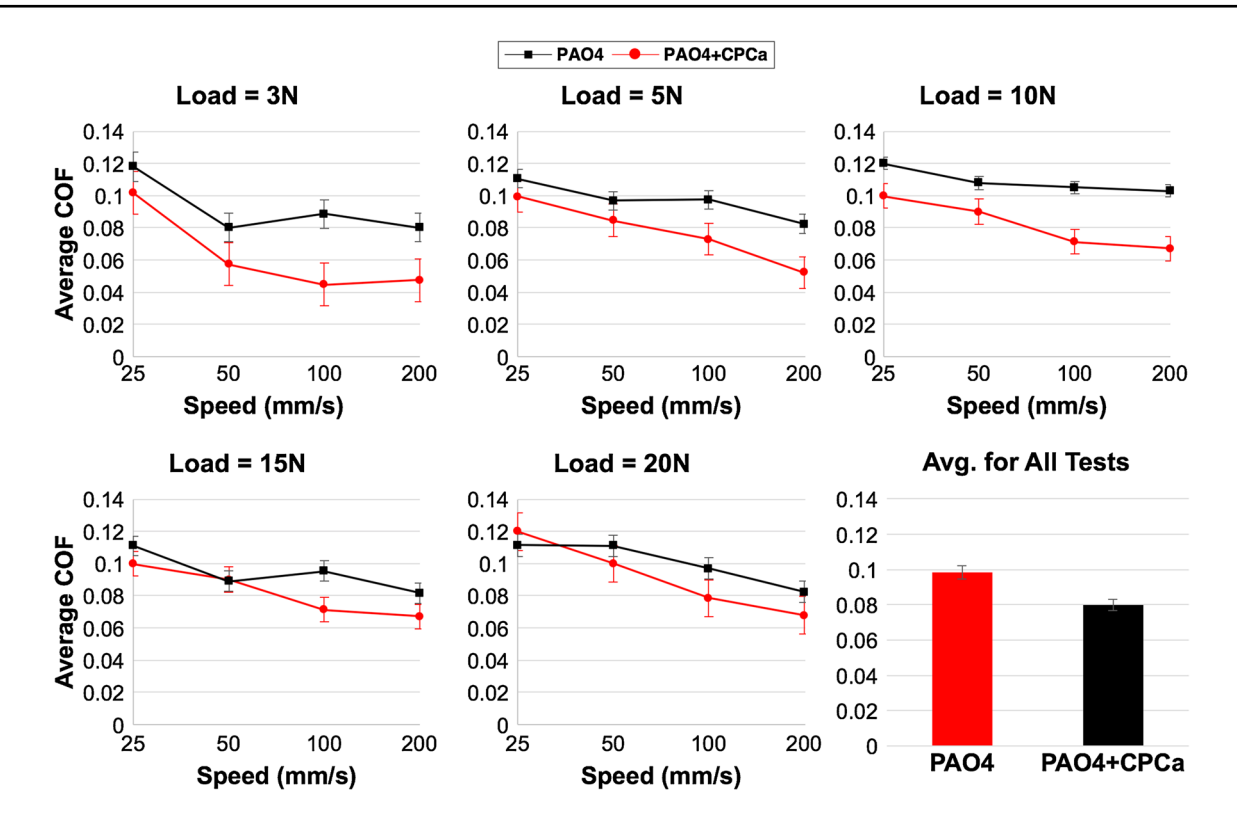


Fig. 5 Time-averaged coefficient of friction for tests using PAO4 and PAO4 + CPCa as lubricants, and a comparison of friction coefficients averaged over all 20 tests using these lubricants

from the untested disk surface, the wear scar, a commercial DLC film, and the colored deposit. This comparison identifies the deposit as DLC-like carbon tribofilm, which is present only in samples tested with PAO4 + CPCa. Its adhesion to the disk surface is not strong, as we can remove it after 5-min sonication in hexane.

Figure 9 shows a series of SEM images obtained from the disk surface after testing at 200 mm s⁻¹ and 10 N. Figure 9a shows two wear tracks: one after testing in PAO4 and one in PAO4 + CPCa. The streaks of dark material on the bottom wear scar were previously identified as a DLC-like material using Raman spectroscopy. Figure 9b shows a more detailed look, revealing the flaky appearance of the carbon material generated within the wear scar. The material is similar in appearance to DLC transfer layers previously reported [60]. Figure 9c, d shows the smearing of the film across the surface, filling in crevices and smoothing rough areas.

Cross-sectional SEM images were also obtained using FIB milling on a disk that was lubricated with base oil and 2.5 wt% CPCa under 10 N and 200 mm s⁻¹. Figure 10 shows an SEM image taken at an approach angle of 52°, after milling. Before milling, a palladium overlayer was sputtered onto the surface to protect it from damage. A line scan of EDS elemental analysis was performed across the boundary of the overlayer and the steel surface, revealing a carbon-rich

tribofilm that is visible in the dark regions between the overlayer and the steel.

Figure 11 shows Raman spectra obtained from the posttest ball surface for a variety of loading and speed conditions tested with PAO4 + CPCa. The broad peak from 400 to 900 cm⁻¹ appears on all samples, likely due to surface oxides and/or oxide wear particles [61]. Just outside the contact area, carbon films formed are thick enough to be readily detectable by Raman spectroscopy (D peak around 1350 cm⁻¹ and G peak around 1600 cm⁻¹) as noted by previous authors [31, 62]. All D/G ratios fall between 0.25 and 0.45, indicating an amorphous carbon material similar to nanocrystalline graphite [21]. Visual inspection shows that the D/G ratio increases with increasing speed and load, consistent with previous observations made of carbon transfer layers from DLC coatings [21, 62]. Also note the shift of the G peak from carbon tribofilms formed in our experiments to higher wavenumbers compared with the DLC reference sample. This shift is attributed to increased fraction of sp²-bonded carbon, indicating that carbon tribofilms formed in these experiments are more graphitic than the commercial DLC [60].

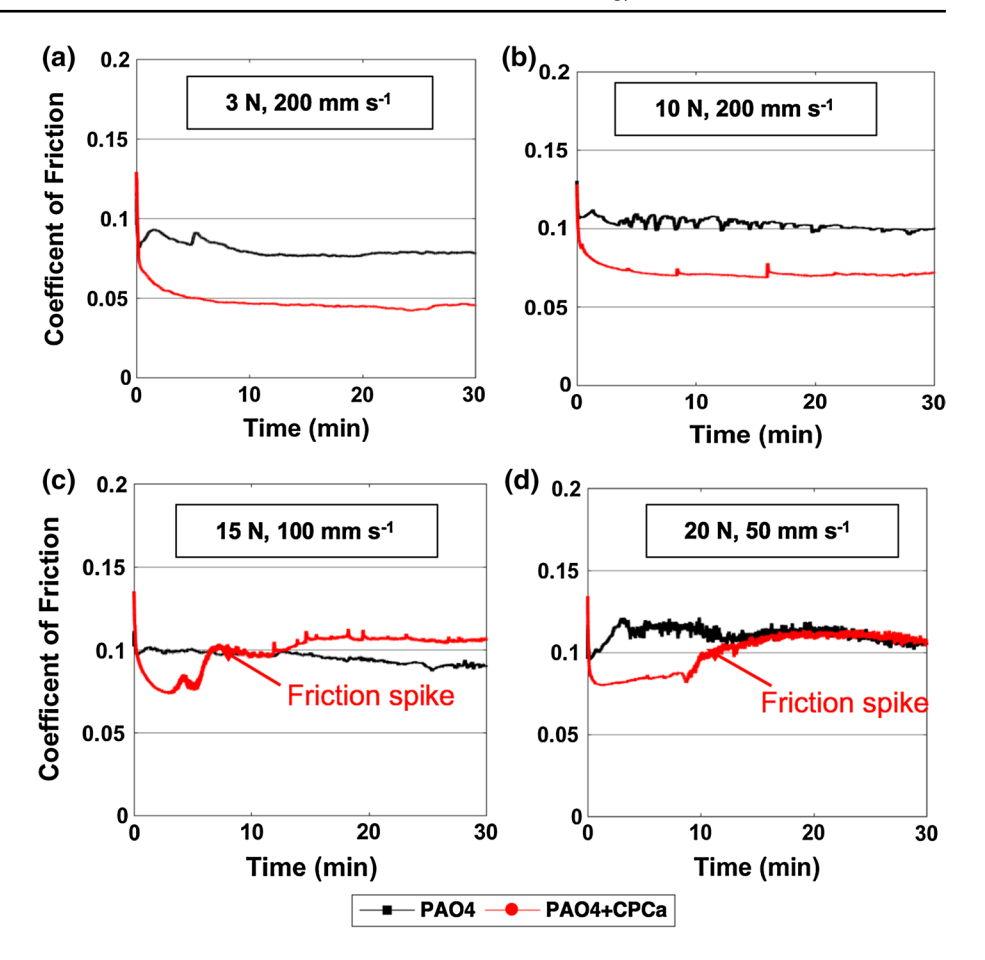
Figure 12 shows two optical micrographs of the ball surface tested with PAO4 + CPCa at 15 N load and a speed of 100 mm s⁻¹. This test condition yields a friction jump after about 10 min into the test as shown in Fig. 6c. Repeated tests



Page 6 of 13 Tribology Letters (2018) 66:2

Fig. 6 Selected friction—time curves, showing initial rapid friction reduction (**a**, **b**), in the presence of CPCa, and in some cases, followed by sudden friction increase, as noted in **c** and **d**

X



were stopped before and immediately after the friction jump, so that images of the ball surface could be taken. Figure 9a shows that before the friction jump, the surface contains a dark, mostly continuous tribofilm in the outlet area that has about the same width as the contact. Figure 9b shows that after the friction jump, the film has become thinner and discontinuous.

4 Discussion

4.1 Tribochemical Mechanisms

Tribotesting and post-test analysis have demonstrated the in situ tribochemical transformation of CPCa into a carbon tribofilm that provides friction reduction and wear protection. Through the CPCa additive, effective, friction-induced, carbon lubrication is achieved at ambient temperatures, with no catalyst required. These observations suggest that carbon tribofilms are formed from the carbon precursor additive, as shown in Fig. 10. Once added to a lubricant, the precursor additive adsorbs onto the mating surfaces (Fig. 13a). At asperity contacts, the high flash temperature

and pressure trigger fragmentation of the metastable cycloal-kane (Fig. 13b), which eventually results in the formation of carbon tribofilms (Fig. 13c). Their relative softness allows the films to be sheared to fill in crevices. These tribofilms are similar to previously reported graphitized DLC transfer layers in appearance, Raman signature, and friction performance [30, 31].

These tribofilms are effective in reducing friction and wear as long as the film formation rate is greater than the removal rate by wear. At sufficiently severe tribotesting conditions (e.g., combination of high load and low speed), the tribofilm removal rate is sufficiently high that the tribofilm is depleted from the contact, resulting in the friction jump as shown in Fig. 4c, d.

4.2 Activation Energy

Based on our dataset of friction—time curves under a range of speed and load conditions, we have developed a method to determine the activation energy for carbon tribofilm formation. Steiner et al. [56] presented a model that predicts friction and wear performance of DLC under several cases. The model includes a method for correlating friction reduction



Tribology Letters (2018) 66:2 Page 7 of 13 ☑

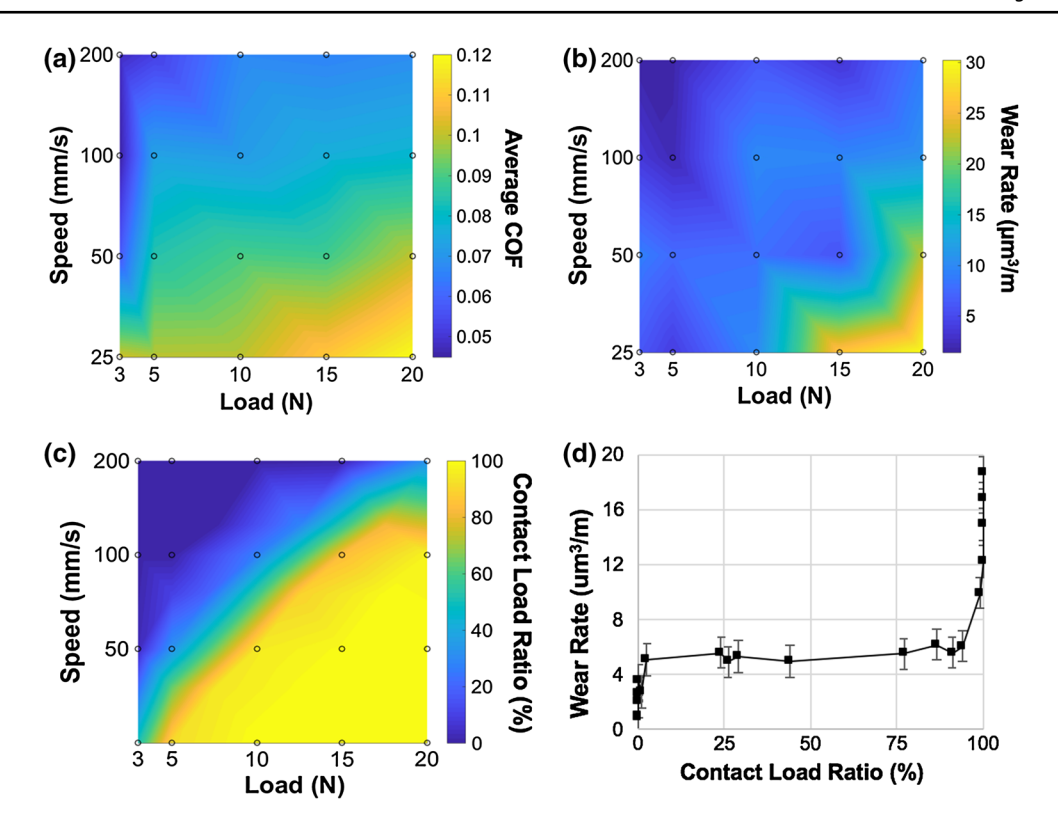
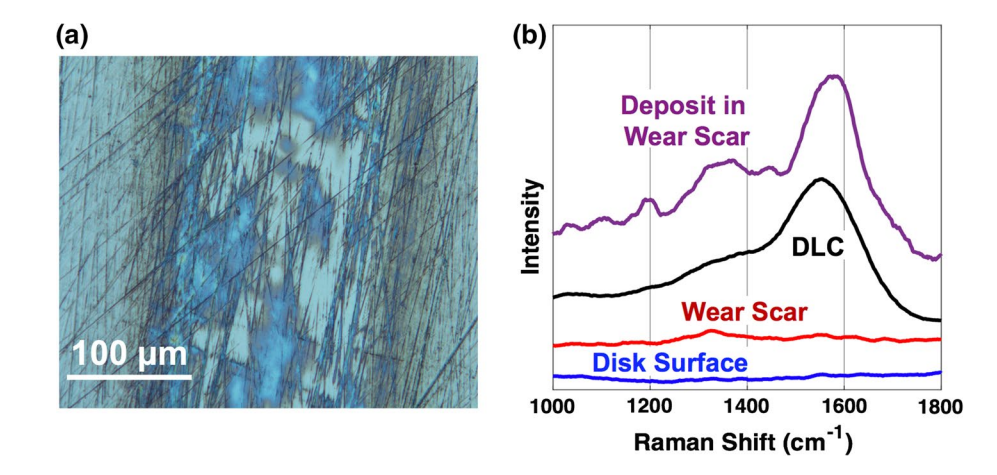


Fig. 7 Interpolated maps of $\bf a$ friction and $\bf b$ wear results based on tests using PAO4 + CPCa, $\bf c$ interpolated map of contact load ratio (%), and $\bf d$ variation of wear rate as a function of contact load ratio. Black circles mark the load speed combinations of the 20 tests

Fig. 8 a Optical micrograph obtained from the disk surface after tribotesting at 10 N and 200 mm s⁻¹ with PAO4 + CPCa, and **b** Raman spectra obtained from a wear scar (with and without the deposit) from the same test, a commercial DLC film, and an untested disk surface



with carbon tribofilm growth. It is based on the assumption that during contact, newly formed graphitic carbon accumulates inside roughness grooves of the surfaces, and friction is continually reduced until the roughness grooves are filled and coefficient of friction (COF) reaches a steady-state value. Under this assumption, the difference in friction between the neat PAO4 sample and the PAO4 + CPCa sample can be connected to the thickness of carbon filling in the surface roughness, as shown below

$$\mu(t)_{PAO4+CPCa} \approx \mu_{PAO4}^{SS} - \frac{D_C}{R} \Delta \mu^{SS} \tag{1}$$

where D_C is the thickness of the carbon tribofilm formed within the contact area, $\Delta \mu^{SS}$ the difference in the COF at the steady state for the PAO4 and PAO4 + CPCa samples, and R the surface roughness of the rougher surface. Figure 11 shows these variables graphically for the 3 N, 100 mm s⁻¹ experiment.

Additionally, the friction curve for PAO4 + CPCa in Fig. 14 can be approximated with an exponential decay function, as shown below:

$$\mu(t)_{PAO4+CPCa} \approx \Delta \mu^{SS} e^{-\lambda t} + \mu_{PAO4+CPCa}^{SS}$$
 (2)



Page 8 of 13 Tribology Letters (2018) 66:2

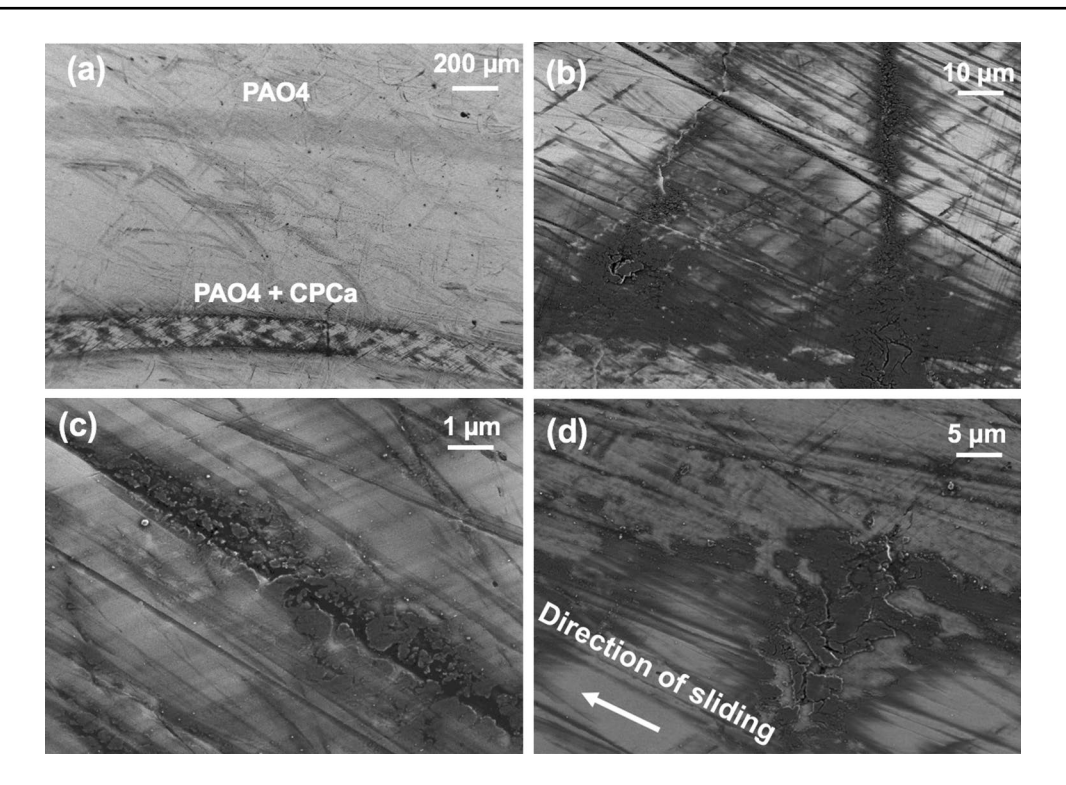
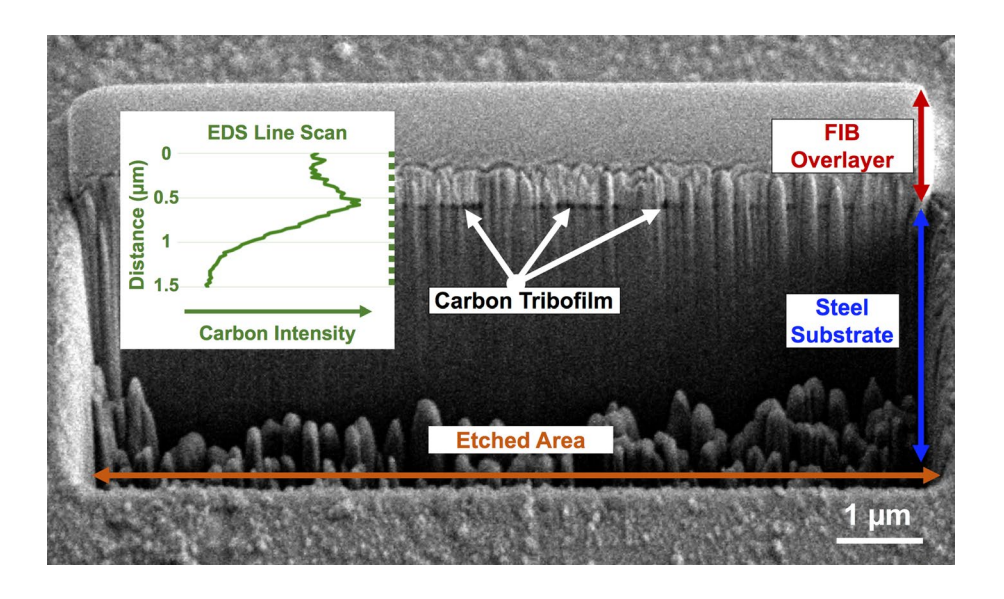


Fig. 9 a SEM image of the post-test disk, lubricated with PAO4 and PAO4 + CPCa; more detailed view of the wear track tested with PAO4 + CPCa, showing $\bf b$ the formation of flakes, $\bf c$ the carbon film filling in crevices, and $\bf d$ smearing of the film along direction of sliding

Fig. 10 Cross-sectional SEM image of a post-test disk surface etched away using FIB milling, revealing the dark carbonaceous regions on the steel surface, with the protective palladium overlayer. The elemental analysis line scan for carbon is included across the surface boundaries

X



where λ is the exponential decay constant and t time of the experiment. Setting Eq. (1) equal to Eq. (2), we can solve for the carbon tribofilm thickness D_C :

$$D_C = R(1 - e^{-\lambda t}) \tag{3}$$

write $t_{1/2}$ as the time it takes for carbon to fill in half of the surface roughness. It can be readily shown that $t_{1/2} = \ln 2/\lambda$. We approximate the average growth rate of carbon k as the growth rate at $t = t_{1/2}$:

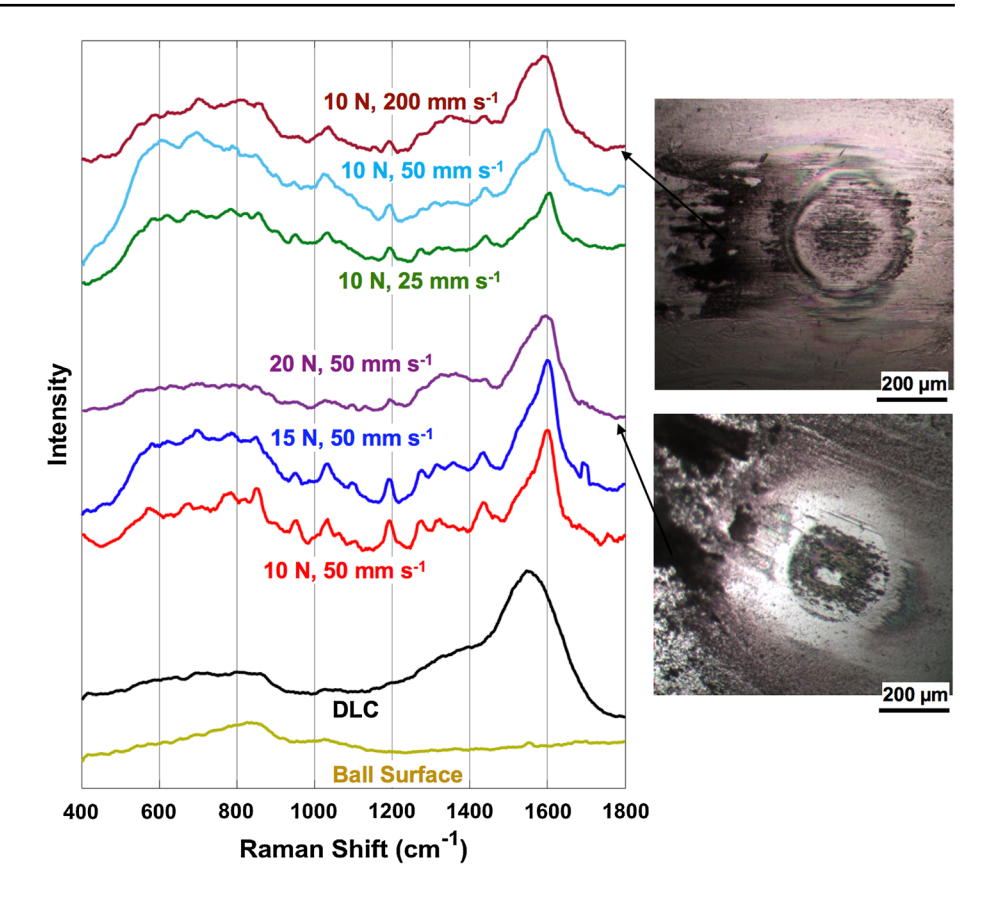
$$k = \left(\frac{dD_C}{dt}\right)_{t=t_{1/2}} = \frac{R \ln 2}{2t_{1/2}} \tag{4}$$

The Arrhenius plot is then constructed by plotting $\ln k$ versus the inverse of the flash temperature T^{-1} for each tribotest. A collection of these Arrhenius plots is shown in Fig. 15a for each testing load. For most tribochemical reactions, including reactions involving carbon [30], shear stress



Tribology Letters (2018) 66:2 Page 9 of 13 ☑

Fig. 11 Raman spectra obtained from ball surfaces after testing with PAO4 + CPCa, along with spectra from untested DLC and ball surfaces



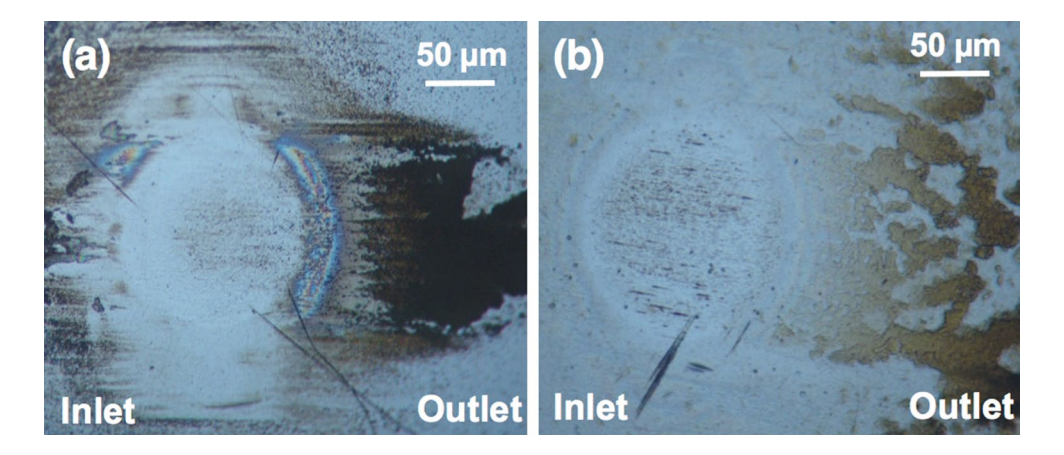


Fig. 12 Optical micrographs of the ball surface after testing with PAO4 + CPCa test at 15 N and 100 mm s⁻¹ (a) before the jump in friction, and b immediately after the jump in friction

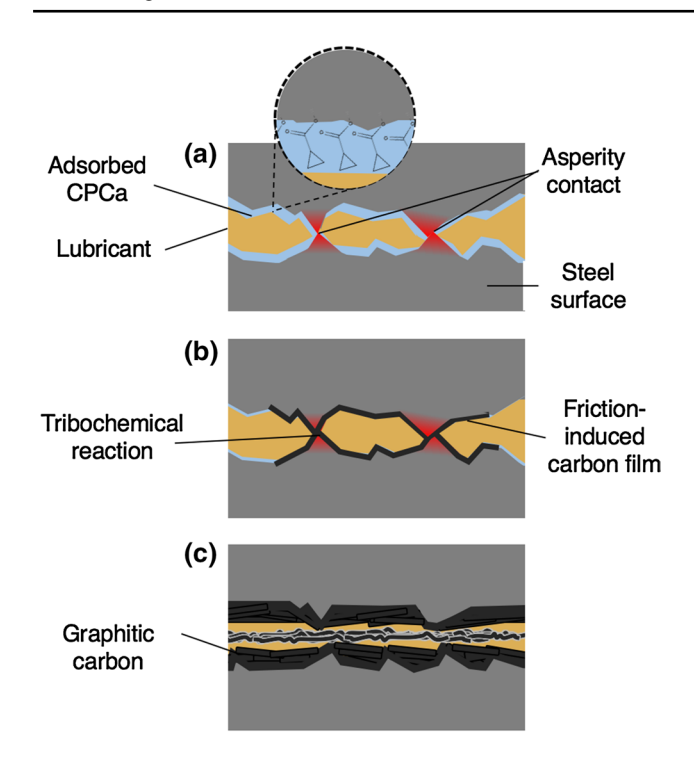
decreases the activation energy barrier for the reaction [33, 63–66], thus accelerating the tribochemical reaction. We can then express the carbon tribofilm growth rate k as a function of stress σ as follows:

$$k = k_o \exp\left(-\frac{\Delta E_{act}}{k_b T}\right) \tag{5}$$

where $\Delta E_{act} = \Delta E_{act,o} - \sigma V_{act}$, ΔE_{act} being the activation energy with contact pressure, $\Delta E_{act,o}$ activation energy without motion, σ the shear stress, k_o the pre-exponential factor, k_b Boltzmann constant, T absolute temperature, and ΔV_{act} the activation volume [66, 67]. Here, the activation volume depends on the effects of stress (including shear) on molecular deformation, not the physical volume of the molecule. Shear stress was approximated by multiplying the normal contact stress by the steady-state coefficient of friction from



Page 10 of 13 Tribology Letters (2018) 66:2



X

Fig. 13 Mechanism of carbon formation from CPCa. **a** CPCa molecules adsorb on mating surfaces, **b** high flash temperature and pressure trigger tribochemical reaction that produces the carbon tribofilm, and $\bf c$ soft carbon tribofilm filling in the surface roughness

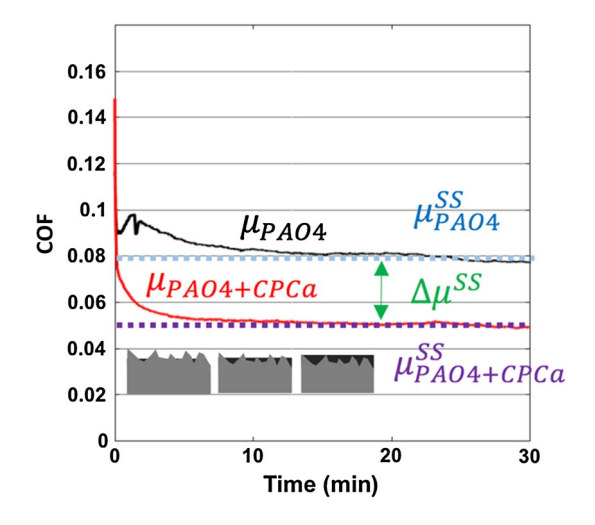


Fig. 14 An example (3 N, 200 mm s^{-1}) of the COF-time curve that demonstrates the difference between the PAO4 and PAO4 + CPCa samples attributed to carbon tribofilm formation

each test [68]. For each shear stress, we can determine ΔE_{act} from the Arrhenius plot in Fig. 15a based on Eq. (5). Figure 15b shows how ΔE_{act} varies with shear stress. From these results, we determine the activation energy under zero stress to be 223.5 kJ/mole, which compares very well with the

reported value for C–C bond dissociation within cyclopropane (257 kJ/mole) [69], and also the dissociation energy of CPCa estimated from the decomposition temperature (249 kJ/mole) [70]. This match supports the hypothesis that the opening of the cyclopropane ring is the rate-determining step in carbon tribofilm formation from the decomposition of CPCa.

5 Conclusions

We demonstrated a novel technique for carbon tribofilm lubrication using cyclopropanecarboxylic acid (CPCa), a carbon precursor additive molecule that dissolves in oil, adsorbs on contact surfaces, and undergoes a tribochemical transformation into a lubricious graphitic tribofilm. The major conclusions of this study are:

- For all tests, the addition of 2.5 wt% of CPCa to PAO4
 results in an average 18% reduction in friction and 93%
 reduction in wear rate under boundary and mixed lubrication regimes.
- SEM images of the post-test surfaces show that carbon is generated near areas of high asperity contact, filling in rough areas of the surface. The tribofilm is also sheared across the surface in the direction of sliding.
- Raman spectroscopy confirmed that the tribofilm consists of a relatively soft and amorphous graphitic material.
 More graphitized carbon is linked to better tribological performance.
- The activation energy of carbon tribofilm formation was determined to be 223.5 kJ mol⁻¹, which is close to the C-C bond dissociation energy in cyclopropane within CPCa.
- This study suggests a new strategy to providing replenishable carbon films for on-demand lubrication without resorting to special surface modification methods.

Acknowledgements The authors would like to thank the support from the US National Science Foundation (Grant No. CMMI-1662606) and Northwestern University (the McCormick Research Catalyst Awards Fund Grant No. 10038293). This work made use of the Keck-II Facility of Northwestern University's NUANCE Center, which has received support from the Keck Foundation, the Soft and Hybrid Nanotechnology Experimental (SHyNE) Resource (NSF ECCS-1542205), the Materials Research Center (NSF DMR-1121262), the McCormick Research Catalyst Awards Fund, Grant No. 10038293, and the International Institute for Nanotechnology (IIN) at Northwestern University. Hongxing Wu would also like to acknowledge the scholarship support from China Scholarship Council (CSC, No. 201606280181).



Tribology Letters (2018) 66:2 Page 11 of 13 ☑

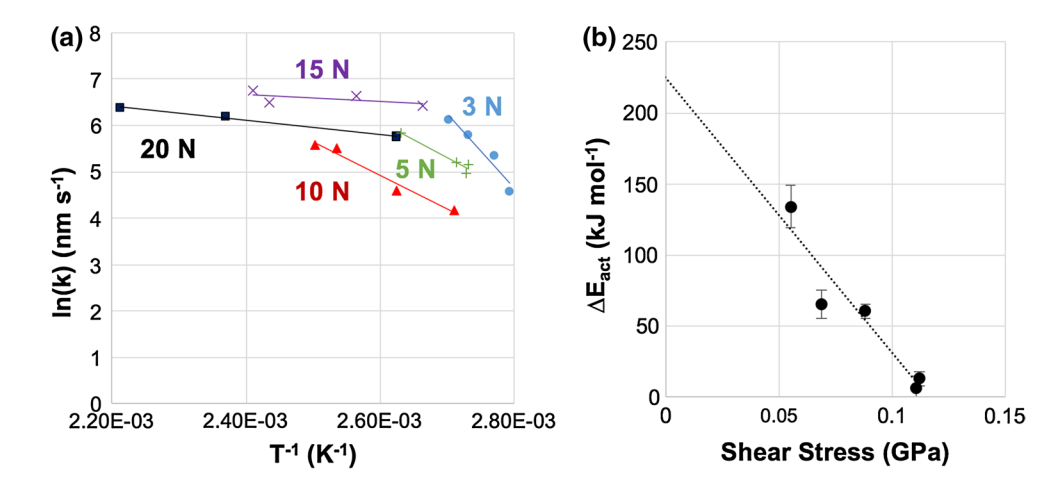


Fig. 15 a Arrhenius plots for different loads, whose slopes correspond to the activation energy of the tribochemical reaction at differing loads; b Relationship between activation energy for tribofilm formation versus shear stress

References

- Holmberg, K., Erdemir, A.: Influence of tribology on global energy consumption, costs and emissions. Friction 5(3), 263–284 (2017). https://doi.org/10.1007/s40544-017-0183-5
- Nosonovsky, M., Bhushan, B.: SpringerLink (Online service): Green Tribology: Biomimetics, Energy Conservation and Sustainability. Green Energy and Technology. Springer, Berlin (2012)
- Holmberg, K., Andersson, P., Nylund, N.-O., Mäkelä, K., Erdemir, A.: Global energy consumption due to friction in trucks and buses. Tribol. Int. 78, 94–114 (2014). https://doi.org/10.1016/j. triboint.2014.05.004
- Holmberg, K., Siilasto, R., Laitinen, T., Andersson, P., Jäsberg, A.: Global energy consumption due to friction in paper machines. Tribol. Int. 62, 58–77 (2013). https://doi.org/10.1016/j.triboint.2013.02.003
- Russell, L.S.D.J.A.: A review of DOE ECUT tribology. J. Tribol. 108(4), 497–501 (1986)
- Holmberg, K., Andersson, P., Erdemir, A.: Global energy consumption due to friction in passenger cars. Tribol. Int. 47, 221–234 (2012). https://doi.org/10.1016/j.triboint.2011.11.022
- Marr, L.C., Kirchstetter, T.W., Harley, R.A., Miguel, A.H., Hering, S.V., Hammond, S.K.: Characterization of polycyclic aromatic hydrocarbons in motor vehicle fuels and exhaust emissions. Environ. Sci. Technol. 33(18), 3091–3099 (1999)
- 8. Jost, H.P.: Tribology—origin and future. Wear **136**(1), 1–17 (1990)
- Jost, H.P., Schofield, J.: Energy saving through tribology: a techno-economic study. Proc. Inst. Mech. Eng. 195(1), 151–173 (1981)
- Bishop, J., Nedungadi, A., Ostrowski, G., Surampudi, B., Armiroli, P., Taspinar, E.: An engine start/stop system for improved fuel economy. In: SAE Technical Paper, (2007)
- Tanaka, K., Korematsu, K., Yamazaki, Y.: Study on intelligent idling stop system. In: 2000 FISITA World Automotive Congress: Automotive Innovation for the New Millennium Seoul, pp. 1–4 (2000)
- Rudnick, L.R.: Lubricant Additives: Chemistry and Applications. CRC Press, Boca Raton (2010)
- Dake, L., Russel, J., Debrodt, D.: A review of DOE ECUT tribology surveys. J. Tribol. 108(4), 497–501 (1986)

- Elo, R., Jacobson, S.: Formation and breakdown of oil residue tribofilms protecting the valves of diesel engines. Wear 330, 193–198 (2015)
- 15. Speed, L.: Engine oils. Engine Professional, pp. 46–47 (2009)
- Guinther, G.H., Danner, M.M.: Development of an engine-based catalytic converter poisoning test to assess the impact of volatile ZDDP decomposition products from passenger car engine oils. In: SAE Technical Paper, (2007)
- Bardasz, E.A.: 26 Crankcase Lubricants. Synthetics, Mineral Oils, and Bio-Based Lubricants: Chemistry and Technology, p. 433 (2013)
- Parekh, K., Mourhatch, R., Aswath, P.: ZDDP-additive-catalyst interactions in engine oil. In: World Tribology Congress III 2005, pp. 661–662. American Society of Mechanical Engineers
- Grill, A.: Review of the tribology of diamond-like carbon. Wear 168(1–2), 143–153 (1993)
- Grill, A.: Tribology of diamondlike carbon and related materials: an updated review. Surf. Coat. Technol. 94, 507–513 (1997)
- Ferrari, A.C., Robertson, J.: Raman spectroscopy of amorphous, nanostructured, diamond–like carbon, and nanodiamond. Philos. Trans. R. Soc. Lond. A Math. Phys. Eng. Sci. 362(1824), 2477– 2512 (2004)
- Lemoine, P., Quinn, J., Maguire, P., McLaughlin, J.: Mechanical characterisation and properties of DLC films. In: Tribology of Diamond-Like Carbon Films. pp. 83–101. Springer, (2008)
- Chung, Y.-W., Bhatia, S.: Tribological behavior of amorphous carbon nitride overcoats for magnetic thin-film rigid disks. J. Tribol. 118, 543 (1996)
- Kovalchenko, A., Ajayi, O.O., Erdemir, A., Fenske, G.R.: Friction and wear performance of low-friction carbon coatings under oil lubrication. In: SAE Technical Paper, (2002)
- Singer, I.L., Dvorak, S.D., Wahl, K.J., Scharf, T.W.: Role of third bodies in friction and wear of protective coatings.
 J. Vac. Sci. Technol., A 21(5), S232 (2003). https://doi.org/10.1116/1.1599869
- Bull, S.: Tribology of carbon coatings: DLC, diamond and beyond. Diam. Relat. Mater. 4(5–6), 827–836 (1995)
- Haque, T., Morina, A., Neville, A., Kapadia, R., Arrowsmith,
 Study of the ZDDP antiwear tribofilm formed on the DLC coating using AFM and XPS techniques. J. ASTM Int. 4(7), 1–11 (2007)



Page 12 of 13 Tribology Letters (2018) 66:2

 Gupta, P.: Iron-Doped Diamond-Like Carbon Coatings (Fe-DLCs): Synthesis, Characterization, and Tribology. Northwestern University (2016)

- Vlad, M., Szczerek, M., Michalczewski, R., Kajdas, C., Tomastik, C., Osuch-SŁomka, E.: The influence of antiwear additive concentration on the tribological behaviour of aC: H: W/steel tribosystem. Proc. Inst. Mech. Eng. Part J J. Eng. Tribol. 224(10), 1079–1089 (2010)
- Hoffman, E.E., Marks, L.D.: Graphitic carbon films across systems. Tribol. Lett. 63(3), 32 (2016)
- 31. Erdemir, A., Ramirez, G., Eryilmaz, O.L., Narayanan, B., Liao, Y., Kamath, G., Sankaranarayanan, S.K.: Carbon-based tribofilms from lubricating oils. Nature **536**(7614), 67–71 (2016)
- Erdemir, A.A.E.O.,: Tribochemically driven diamond-like carbon boundary films from base lubricating oils. 2013 STLE Annual Meeting (2013)
- Gao, F., Furlong, O., Kotvis, P., Tysoe, W.: Tribological properties of films formed by the reaction of carbon tetrachloride with iron. Tribol. Lett. 20(2), 171–176 (2005)
- Hsu, S., Klaus, E., Cheng, H.: A mechano-chemical descriptive model for wear under mixed lubrication conditions. Wear 128(3), 307–323 (1988)
- Hsu, S.M., Gates, R.S.: Effect of materials on tribochemical reactions between hydrocarbons and surfaces. J. Phys. D Appl. Phys. 39(15), 3128 (2006)
- Yu, Y., Gu, J., Kang, F., Kong, X., Mo, W.: Surface restoration induced by lubricant additive of natural minerals. Appl. Surf. Sci. 253(18), 7549–7553 (2007)
- Yuansheng, J., Shenghua, L.: Superlubricity of in situ generated protective layer on worn metal surfaces in presence of Mg 6 Si 4 O 10 (OH) 8. Superlubricity 447 (2007)
- 38. Yuansheng, J., Shenghua, L., Zhengye, Z., He, Y., Feng, W.: In situ mechanochemical reconditioning of worn ferrous surfaces. Tribol. Int. **37**(7), 561–567 (2004)
- Blanchet, T., Lauer, J., Liew, Y.-F., Rhee, S., Sawyer, W.: Solid lubrication by decomposition of carbon monoxide and other gases. Surf. Coat. Technol. 68, 446–452 (1994)
- Yeon, J., He, X., Martini, A., Kim, S.H.: Mechanochemistry at solid surfaces: polymerization of adsorbed molecules by mechanical shear at tribological interfaces. ACS Appl. Mater. Interface 9(3), 3142–3148 (2017)
- He, X., Barthel, A.J., Kim, S.H.: Tribochemical synthesis of nanolubricant films from adsorbed molecules at sliding solid interface: tribo-polymers from α-pinene, pinane, and n-decane. Surf. Sci. 648, 352–359 (2016)
- Faust, R.: Fascinating natural and artificial cyclopropane architectures. Angew. Chem. Int. Ed. 40(12), 2251–2253 (2001)
- de Meijere, A.: Bonding properties of cyclopropane and their chemical consequences. Angew. Chem., Int. Ed. Engl. 18(11), 809–826 (1979)
- Liu, S., Wang, Q.: Studying contact stress fields caused by surface tractions with a discrete convolution and fast fourier transform algorithm. J. Tribol. 124(1), 36–45 (2002)
- 45. Liu, G., Wang, Q., Liu, S.: A three-dimensional thermal-mechanical asperity contact model for two nominally flat surfaces in contact. J. Tribol. **123**(3), 595–602 (2001)
- Liu, Y., Wang, Q.J., Zhu, D., Shi, F.: A Generalized thermal EHL model for point contact problems. In: STLE/ASME 2008 International Joint Tribology Conference 2008, pp. 281–282. American Society of Mechanical Engineers
- Chen, W.W., Wang, Q.J., Kim, W.: Transient thermomechanical analysis of sliding electrical contacts of elastoplastic bodies, thermal softening, and melting inception. J. Tribol. 131(2), 021406 (2009)
- Chen, W.W., Wang, Q.J.: Thermomechanical analysis of elastoplastic bodies in a sliding spherical contact and the effects of

- sliding speed, heat partition, and thermal softening. J. Tribol. **130**(4), 041402 (2008)
- Martini, A., Liu, S., Wang, Q.J.: Transient three-dimensional solution for thermoelastic displacement due to surface heating and convective cooling. J. Tribol. 127(4), 750–755 (2005)
- Zhang, C., Cheng, H., Wang, Q.J.: Scuffing behavior of piston-pin/ bore bearing in mixed lubrication—part II: scuffing mechanism and failure criterion. Tribol. Trans. 47(1), 149–156 (2004)
- 51. Wang, Y., Zhang, C., Wang, Q.J., Lin, C.: A mixed-TEHD analysis and experiment of journal bearings under severe operating conditions. Tribol. Int. **35**(6), 395–407 (2002)
- 52. Bhushan, B., Fuchs, H., Tomitori, M.: Applied Scanning Probe Methods VIII: Scanning Probe Microscopy Techniques. Nanoscience and Technology. Springer, Berlin (2008)
- Erdemir, A., Eryilmaz, O., Kim, S.: Effect of tribochemistry on lubricity of DLC films in hydrogen. Surf. Coat. Technol. 257, 241–246 (2014)
- Totolin, V., Ripoll, M.R., Jech, M., Podgornik, B.: Enhanced tribological performance of tungsten carbide functionalized surfaces via in situ formation of low-friction tribofilms. Tribol. Int. 94, 269–278 (2016)
- Field, S., Jarratt, M., Teer, D.: Tribological properties of graphitelike and diamond-like carbon coatings. Tribol. Int. 37(11), 949– 956 (2004)
- Steiner, L., Bouvier, V., May, U., Hegadekatte, V., Huber, N.: Modelling of unlubricated oscillating sliding wear of DLC-coatings considering surface topography, oxidation and graphitisation. Wear 268(9), 1184–1194 (2010)
- Morina, A., Neville, A.: Understanding the composition and low friction tribofilm formation/removal in boundary lubrication. Tribol. Int. 40(10), 1696–1704 (2007)
- Wang, Y., Wang, Q.J., Lin, C., Shi, F.: Development of a set of Stribeck curves for conformal contacts of rough surfaces. Tribol. Trans. 49(4), 526–535 (2006)
- Jung, I., Rhyee, J.-S., Son, J.Y., Ruoff, R.S., Rhee, K.-Y.: Colors of graphene and graphene-oxide multilayers on various substrates. Nanotechnology 23(2), 025708 (2011)
- Kim, D.-W., Kim, K.-W.: Effects of sliding velocity and normal load on friction and wear characteristics of multi-layered diamond-like carbon (DLC) coating prepared by reactive sputtering. Wear 297(1), 722–730 (2013)
- Farrow, R., Benner, R., Nagelberg, A., Mattern, P.: Characterization of surface oxides by Raman spectroscopy. Thin Solid Films 73(2), 353–358 (1980)
- Ferrari, A.C., Robertson, J.: Interpretation of Raman spectra of disordered and amorphous carbon. Phys. Rev. B 61(20), 14095– 14107 (2000)
- Furlong, O., Gao, F., Kotvis, P., Tysoe, W.: Understanding the tribological chemistry of chlorine-, sulfur-and phosphorus-containing additives. Tribol. Int. 40(5), 699–708 (2007)
- Lara, J., Surerus, K., Kotvis, P., Contreras, M., Rico, J., Tysoe,
 W.: The surface and tribological chemistry of carbon disulfide as an extreme-pressure additive. Wear 239(1), 77–82 (2000)
- Spikes, H., Tysoe, W.: On the commonality between theoretical models for fluid and solid friction, wear and tribochemistry. Tribol. Lett. 59(1), 21 (2015)
- Tysoe, W.: On stress-induced tribochemical reaction rates. Tribol. Lett. 65(2), 48 (2017)
- Gosvami, N., Bares, J., Mangolini, F., Konicek, A., Yablon, D., Carpick, R.: Mechanisms of antiwear tribofilm growth revealed in situ by single-asperity sliding contacts. Science 348(6230), 102–106 (2015)
- 68. Hirani, H.: Fundamentals of Engineering Tribology with Applications. Cambridge University Press, Cambridge (2016)
- Anslyn, E.V., Dougherty, D.A.: Modern Physical Organic Chemistry. University Science Books, Sausalito, CA (2006)



Tribology Letters (2018) 66:2 Page 13 of 13 ☑

70. Steele, W., Chirico, R., Knipmeyer, S., Nguyen, A.: Measurements of vapor pressure, heat capacity, and density along the saturation line for ϵ -caprolactam, pyrazine, 1, 2-propanediol, triethylene

glycol, phenyl acetylene, and diphenyl acetylene. J. Chem. Eng. Data **47**(4), 689–699 (2002)

